This version is available at http://strathprints.strath.ac.uk/47206/

Techno-economic investigation of alternative propulsion plants for Ferries and RoRo ships

George A. Livanos[a*], Gerasimos Theotokatos[b], Dimitrios-Nikolaos Pagonis[a]

[a]*Department of Naval Architecture, Ag. Spyridonos Street, Egaleo GR 12210, Greece*

[b]*Department of Naval Architecture & Marine Engineering, 100 Montrose Street, Glasgow G4 0LZ, UK*

Abstract

In this paper, the main alternative propulsion plants based on reciprocating internal combustion engines of a ferry or RoRo ship operating in routes that include Emission Control Areas (ECAs) are comparatively assessed. Specifically, a dual fuel engine propulsion plant is compared with a conventional Diesel engine plant. For both cases, the installation of a Waste Heat Recovery system, which covers a part of the ship electric energy demand, is also considered. The ship main DF engines are assumed to operate using LNG and a small amount of MDO for initiating combustion, whereas low sulphur MDO was regarded as the fuel for the case of the Diesel engine plant. The installation of selective catalytic reduction (SCR) after-treatment unit for reducing the NOx emissions for the case of Diesel engines plant is also taken into account. The propulsion plants were modelled under steady state conditions, and the simulation results were analysed in order to compare the alternative configurations. Furthermore, the energy efficiency design index (EEDI) values were calculated and the two examined propulsion system cases were compared on EEDI basis. Finally, the Life Cycle Cost for each alternative propulsion plant was calculated and used for completing an economic evaluation of the Dual fuel propulsion plant versus the conventional designs applied in ferries.

Keywords: Ferries propulsion plant, Dual fuel engines, waste heat recovery systems, EEDI, techno-economic assessment

1. Introduction

The increased pressure for greener shipping resulted in an updated legislation framework set by the International Maritime Organization (IMO), for constraining the greenhouse gaseous emissions, mainly the carbon dioxide, as well as the nitrogen oxides (NOx) and sulphur oxides (SOx). Thus, in the recent amendment of IMO rules [1-3], the Energy Efficiency Design Index (EEDI) and the Ship Energy Efficiency Management Plan (SEEMP) were introduced focusing on the reduction of CO_2 emissions and fuel consumption throughout the ship lifetime. For reducing SOx emissions, the IMO [4] defines the upper limits of the sulphur content for the fuels used onboard ships sailing inside and outside Emission Control Areas (ECA). Presently, the use of marine fuels with up to 1% sulphur content is only permitted inside ECAs, whereas the allowed fuel sulphur content value will be drastically reduced reaching 0.1% from 2015 onwards. For the NOx emissions, the three tier program [5] has been established according to which, Tier II that requires 15% reduction of NOx compared to Tier I is currently in effect, whereas Tier III imposes 80% reduction in NOx (also compared to Tier I) and will come into effect possibly in 2016.

To cope with the continuously increasing environmental demands, a number of measures for the ship propulsion system can be taken; these comprise the induction of more optimised propulsor designs including wing thrusters and contra rotating propellers, as well as the replacement of the conventional mechanical system by the more flexible Diesel-Electric propulsion system or combined Diesel mechanical/electric propulsion systems [6]. However, in order for the ship propulsion engines running on Heavy Fuel Oil (HFO) or Marine Diesel Oil (MDO) to comply with the future environmental regulations [7], techniques such as Selective Catalytic Reduction (SCR) or Exhaust Gas Recirculation (EGR) might be required for reducing the NOx emissions, whereas exhaust scrubbers or alternatively separate low sulphur fuel systems have to be installed onboard for addressing the SOx emissions reduction issue [8-9]. These measures deteriorate the ship propulsion plant efficiency and as a result increase the CO_2 emissions as well as the ship operational cost. All the above, in conjunction with the unprecedented rising of fuel oil prices throughout the last years and the continuously increasing availability of natural gas resources around the globe [10] render the use of Liquefied Natural Gas (LNG) as an alternative marine fuel attractive. LNG fuel is presently established as a clean and reliable fuel for propulsion and auxiliary power generation and its usage forms a very efficient way for reducing emissions [11]. Indeed, the SOx emissions are totally eliminated owing to the fact that sulphur is not contained in LNG, whereas the NOx emissions can be reduced up to 85% owing to the fact that the combustion takes place at air–fuel ratio values around 2.1 to 2.3 (lean burn combustion concept). In addition, the reduction of CO_2 emissions can reach 25%-30% thanks to the low carbon to hydrogen ratio of fuel. On top of the above, the DF engines exhibit very low particulate emissions level, no visible smoke and no sludge deposits [12]. The LNG infrastructure has been developed in the last years [13], particularly in Norway, to the extent that other ship types, like Ro-Ro and smaller ferryboats can be bunkered.

The use of liquefied fuels (LNG/LPG) for the ship propulsion is not a new idea; these fuels have been used for many years onboard liquefied gas carriers equipped with steam turbine propulsion systems. Recently, four-stroke diesel mechanical or diesel-electric propulsion systems [14] have been also used. The former provide greater increase of the propulsion plant efficiency, whereas the latter combine the high efficiency with the increased flexibility. In all these cases, the boil-off gas produced due to evaporation inside the ship cargo tanks has been used as the main fuel in the ship propulsion system.

Nowadays, the commercial available gas engine portfolio includes three main technologies [15]: Gas, Gas-Diesel (GD), and Dual-Fuel (DF) engines. Gas engines are of the four-stroke type and run exclusively on gas. The combustion of the gas-air mixture takes place based on the Otto cycle triggered by spark plug ignition, whereas the gas is injected into the engine cylinder ports upstream the engine valves at low pressure (4–6 bar). The GD engines can operate on different mixtures of gas and diesel fuels or alternatively on diesel fuel only. The engine cylinder processes follow the Diesel cycle (compression–ignition) and the gas is injected into the engine cylinder during the compression stroke at high pressure (up to 300 bar). These engines could be either of the two-stroke or four-stroke type. Dual Fuel engines are of the four-stroke type and can run in gas or diesel modes. In the gas mode, 99% of the fuel is gas and 1% (the pilot fuel) is diesel fuel. The gas is injected into the engine ports at low pressure (4–6 bar), whereas the combustion of the gas-air mixture takes place following the Otto cycle with the ignition being triggered by the injection of the pilot diesel fuel. In the diesel mode, the fuel is exclusively of the diesel type and the combustion of the diesel-air mixture takes place according to the Diesel cycle. An alternative categorisation of gas fuelled engines can be accomplished based on the ignition principle (spark ignition versus liquid fuel pilot ignition) and the combustion chamber geometry (single chamber versus pre-chamber) [16]. The concept of using DF medium speed diesel engines in marine propulsion plants is continuously expanding nowadays [17]; a number of ferries with DF engines were set in operation in the area of Baltic Sea and new ferries are being designed for operating in the Mediterranean Sea.

One of the most important issues addressed by the classification societies rules is the placement of the LNG tanks; they are not allowed to be close to the vessel sides and must also be at a certain distance above the ship bottom for safety reasons in case of ship grounding. The following locations have been proposed [18-19]: a) in the centre of superstructure, inside the outer raw of cabins and in front of the engine casing but above the public space decks so as not to obstruct the passenger flows, b) down on the tanktop in the centre of the vessel inside the B/5 lines (B: ship breadth), c) in the ship stern, below the swimming pool, and d) on the upper open deck if space available. Another challenge for LNG storage comes from the larger size of the tanks [7]. In order to produce the same amount of energy, a volume of LNG equal to 1.8 times that of diesel fuel is required. When taking into account the LNG tank insulation volume and the maximum tank filling ratio that can be only up to 95%, the required volume is increased to about 2.3 times compared to the respective in the case of diesel fuel. The practical space required in the ship becomes about 4 times higher when also counting the squared void

space around the cylindrical LNG tank. If compared to the MDO tanks located above the ship double bottoms, the total volume difference is somewhat smaller, about 3 times. The weight of the bunkered LNG amount is marginally lower than that of MDO, when considering the actual fuel itself. However, the special tank and tank room steel structure increases the total weight for LNG storage to about 1.5 times higher than the respective one required for MDO [18-19].

For further improving the ship power plant efficiency and thus, reducing the fuel consumption and CO_2 emissions, waste heat recovery (WHR) systems have been used. Depending on the ship size, the following typical options of the exhaust gas WHR systems are commonly installed [20-22]: a) systems for the production of saturated steam indented for covering the thermal power requirements of the ship (heating services), b) systems for generating electricity in a steam turbine driven generator (turbo-generator), and (c) system generating electric energy in a combined steam turbine/power gas turbine driven generator. A comprehensive review of the waste heat recovery applications for oceangoing vessels is presented in [23]. In Dimopoulos et al [24] the modelling and optimisation of a containership power plant system combined with a waste heat recovery system was presented. In Hountalas et al [25], the waste heat recovery system for recovering energy from the exhaust gas of a marine two-stroke engine is investigated comparing its obtained performance when using two different working fluids. In Choi and Kim [26], a combined water-organic fluid waste heat recovery system for the propulsion engine of a containership is examined. In Gewald et al [27], an integrated approach to optimise the combined cycle overall system efficiency for three large medium speed engines was presented focusing on the waste heat recovery cycle combined with the optimal layout of the engine cooling system. In Burel et al [28], the power plant of a handy size tanker operating with LNG and for various alternatives of waste heat recovery systems including steam and organic fluid cycles was studied.

Techno-economic investigation of alternative options for propulsion plants, specifically for ships operating frequently in ECA areas, e.g. Ferries, Ro-Ro ships, handy size tankers, is a useful tool that can delineate the cost-effective and environmental sound solutions. Such a study for the propulsion plant of two different ferries was reported in [18], whereas a techno-economic study for a bulk carrier propulsion system was presented in [29]. However, studies for the integrated technical-environmental and economic assessment of gas fuelled engines combined with waste heat recovery systems for ship propulsion plants have not been reported. In that respect, the present study focuses on the investigation of techno-economic and environmental sustainability of four alternative propulsion plants, based on reciprocating internal combustion engines running either on Diesel or LNG fuels, equipped or not with waste heat recovery system for the case of a typical ferry ship operating in routes that include Emission Control Areas (ECAs).

2. Description of investigated propulsion system

The propulsion system of the new built ferries should comply with the maritime regulations, provide increased reliability and safety and additionally operate at high efficiency levels. The typical ferry propulsion system arrangement comprises two pairs of engines of the four-stroke type, which are connected to the respective gearboxes for driving the two ship propellers. A power take-off machine, usually an electric generator, is also connected to each gearbox. The ship electric power demand is covered by a number (usually three electric generators). For further increasing the efficiency and the flexibility of the traditional ferry propulsion system, modified configurations of combined diesel-electric and diesel-mechanical systems, which drive controllable pitch propellers, pod thrusters or contra-rotating propellers have been proposed [6]. For the cases of ferries propulsion plants operating on HFO, SCR units and SOx scrubbers are required in order for the ships to comply with the IMO imposed emissions limits when sailing inside ECAs. The alternative to that option is the use of MGO or MDO inside ECAs and switching to HFO outside ECA zones. However, the installation of a SCR unit is still required for reducing NOx emissions in that case. The third option is the installation of DF engines and the usage of LNG fuel for the ship main engines and generator sets.

In the present work, the power plant system diagrammatically depicted in Figure 1 is investigated. That type of propulsion plant can be found in small to medium size ferries. The propulsion system consists of two main engines of the four-stroke type; each one is connected to one engine controllable pitch propeller via a gearbox unit. In addition, three generator sets are installed for covering the ship electric power requirements. For increasing the efficiency of the power plant at ship sailing conditions, the installation of WHR systems for recovering part of the ship main engines exhaust gas heat and producing electric energy was also studied.

The considered WHR systems arrangement as well as their components and piping are illustrated in Figure 2. The systems are of the single steam pressure type with external heat exchanger for heating the feed water entering into the boiler drum. The heat exchanger is used, so that the water entering the economiser section of the boiler is kept in a temperature level around 130°C (for the case of Diesel fuels) in order to avoid condensing of the sulphur oxides contained in the exhaust gas, which causes corrosion of the boiler surfaces. The option of heating the feed water using the engine air cooler is also taken into consideration. The WHR systems are used for the production of only superheated steam, which expands in a steam turbine coupled to an electric alternator, thus generating electricity. The exhaust gas boiler consists of three stages; the economizer (preheater), the evaporator and the superheater. The feed water is pumped by the feed water pump into the water/steam drum, whereas an external heat exchanger is used for preheating it. As an option, the high temperature stage of the engine air cooler could be also used for initially preheating the feed water. The heating medium of the heat exchanger is the saturated water contained in the drum, which is pumped by the economizer circulating water pump, enters the heat exchanger heating the feed water, leaves the heat exchanger with lower temperature and then enters to the economiser section. The circulating water exiting the economizer returns to the drum having temperature approximately equal to the saturation temperature corresponding to the drum operating pressure. An additional circulating pump is used to circulate the

water through the evaporation section of the boiler, where a portion of saturated water is evaporated and saturated steam is produced. The flow rate of this pump is usually selected two to four times the flow rate of feed water, so that the integrity of the evaporator is not jeopardized in the case where temporarily more steam is produced at system transients. The saturated water/steam mixture exiting the boiler returns into the drum, where the saturated steam is separated from the water and is accumulated in the upper part of the drum. The saturated steam is advanced into the superheater section of the boiler. The superheated steam exiting the boiler enters into the steam turbine stages of turbogenerator, where it expands producing mechanical power and driving the electric generator. The steam exiting the steam turbine is advanced to the condenser, where it condenses by the usage of sea water. The condensate is then pumped into the feed water tank (hot well) through the condensate pump. In case where surplus amount of saturated steam is produced, it is also forwarded into the surplus steam condenser where it converts to condensate water, which subsequently is pumped to the feed water tank.
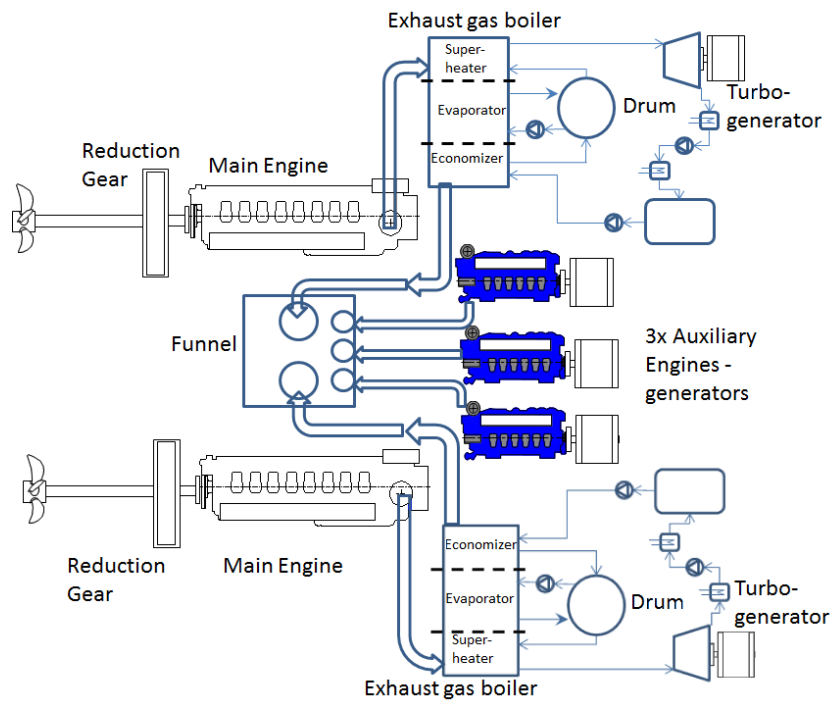

Figure 1. Investigated Ship Propulsion Plant consisting of two main engines (Diesel or Dual-Fuel) and a WHR systems for electric power generation
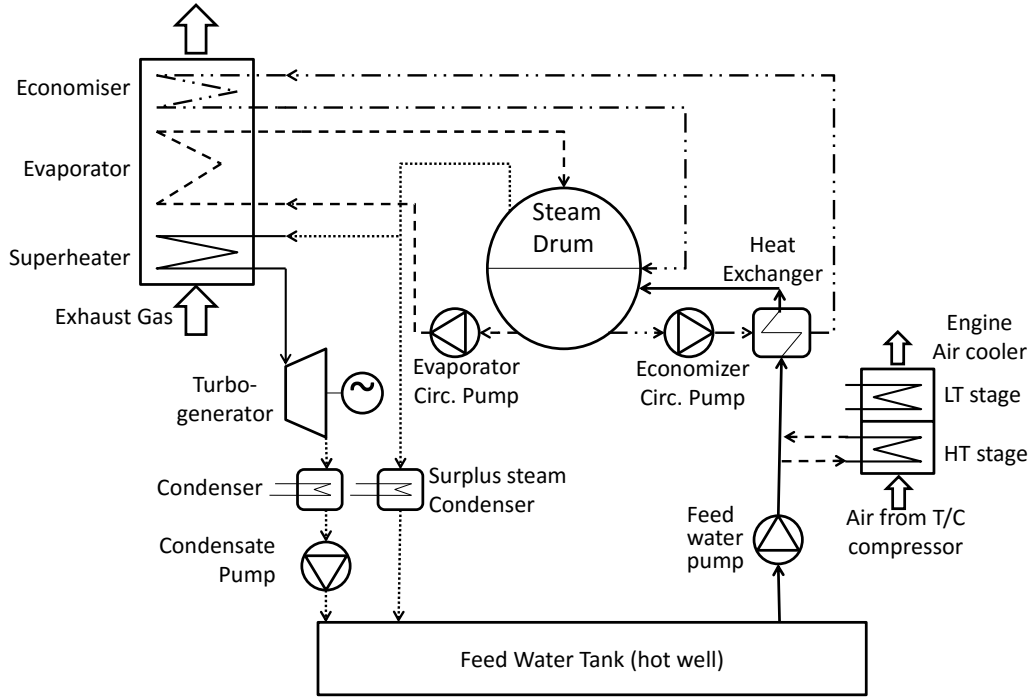
Figure 2. Single steam pressure Waste Heat Recovery System with external heat exchanger

3. Propulsion system modelling

For analysing the engine steady state performance as well as transient response, various modelling techniques have been used; these include mean value engine models [30], zero/one dimensional simulation tools [31-32] or a combination of the two techniques [33]. However, the present study is focused on the steady state operation of the described previously ferry propulsion system and the required steady state engine performance parameters for the selected main and auxiliary engines were taken from the respective engine manufacturers project guides. The operation of these engines in the load region from 50% to 100% of maximum continuous rating (MCR) based on power–speed variation according to propeller law was examined.

For the reduction of the exhaust gas NOx emissions to the Tier II levels, a selective catalytic reduction system will be required, which is installed downstream the engine turbocharger and before the exhaust gas boiler. This operates using urea-water solution, which is injected upstream SCR catalyst, evaporates and reacts with the exhaust gas water vapour to form ammonia. Subsequently, the ammonia reacts with the exhaust gas NOx on the catalyst surfaces and molecular nitrogen and water vapour are formed. For the examined cases in this study, the required urea flow rate in L/h is calculated using the following equation, which was derived by using the formula proposed in [9]:

$$\dot{V}_u = (0.0593\,\Delta NOx + 0.0091)\frac{P_b}{c_u} \qquad (1)$$

where P_b is the engine brake power in kW, ΔNOx is the expected reduction of specific NOx emissions in g/kWh and c_u is urea mass fraction percentage of the used urea-water solution.

Although, there is exhaust gas temperature changing from the urea solution injection point till the SCR unit exit (initially the exhaust gas is cooled due the urea-water evaporation; heating of exhaust gas takes places in catalyst surfaces due to the reaction exothermic nature), this was not taken into account.

The WHR systems operation was analysed under steady state conditions by applying the mass and energy conservation equations in the various components of the installation as explained bellow. The boiler transferred heat from the exhaust gas to the steam/water is calculated using the following equation:

$$\dot{Q}_b = \eta_b \dot{m}_g c_{p\_g}(T_{g\_i} - T_{g\_o}) \qquad (2)$$

where $\dot{m}_g$ is the exhaust gas mass flow rate, c_{p_g} is the exhaust gas mean specific heat at constant pressure, T_{g_i} is the temperature of the exhaust gas entering into the boiler, T_{g_o} is the temperature of the exhaust gas exiting the boiler, and η_b is the boiler efficiency that is in the order of 98-99% (1- η_b is the boiler heat transfer losses).

Considering that saturated water exits the economizer section, mixture of saturated water/steam exits the evaporator section and superheated steam exit the superheater section, the energy balance in the boiler gives:

$$\begin{aligned}\dot{Q}_b &= \dot{Q}_{ec} + \dot{Q}_{ev} + \dot{Q}_{sh} \\ &= \dot{m}_{cw\_ec}(h_w - h_{cw\_ec\_i}) + \dot{m}_{cw\_ev}(h_w - h_{cw\_ev\_i}) + \dot{m}_s(h_s - h_w) + \dot{m}_{sh}(h_{sh} - h_s)\end{aligned} \qquad (3)$$

where $\dot{m}_{cw\_ec}$ is the economizer circulating water mass flow rate, $\dot{m}_{cw\_ev}$ is the evaporator circulating water mass flow rate, $\dot{m}_{sh}$ is the superheated steam mass flow rate, $\dot{m}_s$ is the mass flow rate of the saturated steam produced in the evaporator, $h_{cw\_ec\_i}$ is the specific enthalpy of the circulating water entering into the economizer (which is exiting from the external heat exchanger), h_{sh} is the specific enthalpy of the superheated steam exiting the boiler, $h_{cw\_ev\_i}$ is the specific enthalpy of the circulating water entering into the evaporator (exiting the evaporator circulating water pump), h_w and h_s are the specific enthalpies of saturated water and steam, which form the saturated mixtureexiting the evaporator, respectively.

The energy conservation applied to the system water/steam drum, feed water tank and heat exchanger respectively, gives the following equations:

$$(\dot{m}_{cw\_ec} + \dot{m}_{cw\_ev})(h_{cw} - h_w) = \dot{m}_{fw}(h_{fw\_d\_i} - h_w) \qquad (4)$$

$$\dot{m}_{cw\_ec}(h_{cw\_ec\_pd} - h_{cw\_ec\_i}) = \dot{m}_{fw}(h_{fw\_d\_i} - h_{fw\_HE\_i}) \qquad (5)$$

$$\dot{m}_{fw} h_{fw} = \dot{m}_{sh} h_{c\_pd} \qquad (6)$$

where $\dot{m}_{fw}$ is the feed water mass flow rate, h_{cw} is the specific enthalpy of the water contained within the drum, $h_{fw\_d\_i}$ is the specific enthalpy of the feed water entering into the drum (exiting the heat exchanger), $h_{cw\_ec\_pd}$ is the specific enthalpy of the circulating water exiting the economizer circulating water pump (entering the heat exchanger), $h_{fw\_HE\_i}$ is the specific enthalpy of the feed water entering the heat exchanger (for the case of no heating of the feed water in the engine air cooler this coincides to the specific enthalpy of the feed water exiting the feed water pump, h_{fw_pd}), h_{fw} is the specific enthalpy of the feed water contained within the feed water tank, h_{c_pd} is the specific enthalpy of condensate water exiting the condensate pump (entering the feed water tank), respectively.

The heat exchanger effectiveness is defined by the following equation:

$$\varepsilon_{HE} = \frac{h_{fw\_d\_i} - h_{fw\_HE\_i}}{h_{cw\_ec\_pd} - h_{fw\_HE\_i}} \qquad (7)$$

The specific enthalpy of the water exiting the system pumps are calculated as follows:

$$h_{i\_pd} = h_{i\_pu} + P_i / \dot{m}_i \qquad (8)$$

where P_i is the pump power, $\dot{m}_i$ is the pump mass flow rate, h_{i_pu} and h_{i_pd} are the fluid specific enthalpies upstream and downstream the pump, respectively, and $i = fw$ for the feed water pump, $i = cw\_ec$ for the economizer circulating water pump, $i = cw\_ev$ for the evaporator circulating water pump, $i = c$ for the condensate water pump.

The power for each one of the system pumps is calculated based on the pump pressure increase, efficiency and fluid density as follows:

$$P = \dot{m} \Delta p / (\eta \rho) \qquad (9)$$

where Δp_i is the pump pressure increase; η_i is the pump efficiency and ρ_i is the fluid density.

In the case where the high temperature stage of the engine air cooler is used for heating the feed water tank, the energy balance in the air cooler provides:

$$\dot{m}_{fw} (h_{fw\_HE\_i} - h_{fw\_pd}) = \eta_{ac} \, \dot{m}_a \, c_{p\_a} \, (T_{ac\_HT\_i} - T_{ac\_HT\_o}) \qquad (10)$$

where $\dot{m}_a$ is the air mass flow rate entering the engine air cooler, c_{p_a} is the mean specific heat at constant pressure of the air in the high temperature stage of the engine air cooler, $T_{ac\_HT\_i}$ is the temperature of the air entering the high temperature stage of the engine air cooler, $T_{ac\_HT\_o}$ is the temperature of the air exiting the high temperature stage of the engine air cooler and and η_{ac} is the air cooler efficiency that is in the order of 99.5% ($1- \eta_{ac}$ is the air cooler heat transfer losses).

The mass balance in the waste heat recovery system gives:

$$\dot{m}_{fw} = \dot{m}_s = \dot{m}_{sh} \qquad (11)$$

The circulating pumps mass flow rates were calculated by estimating the respective ratio values:

$$\dot{m}_{cw\_ec} = r_{cw\_ec}\,\dot{m}_{fw}, \; \dot{m}_{cw\_ev} = r_{cw\_ev}\,\dot{m}_{fw} \qquad (12)$$

where r_{cw_ev} is the ratio of evaporator circulating water mass flow rate to the feed water mass flow rate and r_{cw_ec} is the ratio of economiser circulating water mass flow rate to the feed water mass flow rate.

The equations (2)-(12) form an algebraic system of equations with unknowns the mass flow rates and specific enthalpies of water and steam. This is solved iteratively using as initial value of the superheated steam mass flow rate the estimation that provides the ideal Rankine cycle consideration as well as the following input: a) the engine exhaust gas mass flow rate, temperature and equivalence ratio as well as the temperature of the air exiting the turbocharger compressor, b) the pressure of the drum water/steam, c) the pressure and temperature of the feed water tank, d) the way of feed water heating (no heating, using saturated steam or using the engine air cooler) e) the pressure losses in the various boiler sections and the piping of the WHR installation, f) the ratio of the economizer circulating water to the produced saturated steam mass flow rates and the ratio of the evaporator circulating water to the produced saturated steam mass flow rates, g) the mass flow rate of saturated steam required for the ship heating services, h) the boiler efficiency, the pumps efficiency, the external heat exchanger effectiveness and the air cooler efficiency, i) the temperature of superheated steam exiting the boiler, j) the temperature drops at various sections of the WHR installation, k) the condenser pressure, and l) the algebraic equations for the calculation of the properties of water/steam, exhaust gas and air.

The WHR system produced electric power is calculated by the following equation:

$$P_{el} = \dot{m}_{sh} AE_{ST} \eta_{TG} f_b f_T f_L \qquad (13)$$

where AE_{ST} is the available specific energy in the steam turbine (corresponds to the steam isentropic expansion), η_{TG} is the efficiency of the turbo-generator, and f_b, f_T, f_L are correction factors for the steam turbine back pressure, steam temperature and steam turbine load, respectively. Data for the estimation of turbo-generator efficiency and the correction factors are given in [34].

The specific enthalpy of the steam exiting the steam turbine and entering the condenser is calculated by:

$$h_{ST\_o} = h_{ST\_i} - \eta_{ST} AE_{ST} \qquad (14)$$

where h_{ST_i} is the specific enthalpy of the saturated steam entering the steam turbine, $\eta_{ST} = \eta_{TG}/(\eta_G\,\eta_m)$ is the steam turbine efficiency, η_G is the generator efficiency, and η_m is the turbogenerator mechanical efficiency.

The steam exiting the steam turbine is condensed by using sea water in the system condenser. The power of the sea water pump was also calculated by using eq. (9). The required sea water mass flow rate is calculated by the following equation, which was derived by applying the energy balance in the condenser:

$$\dot{m}_{c\_sw} = \dot{m}_{sh}(h_{ST\_o} - h_{c\_w})/(c_{p\_sw}\Delta T_{sw}) \qquad (15)$$

where h_{c_w} is the specific enthalpy of the condensate water exiting the condenser, c_{p_sw} is the condenser sea water specific heat, and ΔT_{sw} is the temperature increase of the sea water in the condenser.

For the examined case, where saturated steam is not used for the ship heating services, the increase in the ship propulsion installation efficiency due to the electric power generation is calculated by the following equation:

$$\Delta\eta = (P_{el} - \sum_{pumps} P) / (\dot{m}_f H_L) \qquad (16)$$

where $\dot{m}_f$ is mass flow rate of the engine fuel and H_L is the fuel lower heating value.

The minimum temperature difference (pinch point) is calculated using the following equation, which is derived using the energy balance in the evaporator and superheater sections of the boiler:

$$\Delta T_{pp} = T_{g\_i} - \frac{\dot{Q}_{ev} + \dot{Q}_{sh}}{\eta_b \dot{m}_g c_{p\_g}} - T_s \qquad (17)$$

4. IMO Energy Efficiency Design Index Calculation

The Marine Environmental Protection Committee (MEPC) of the IMO [2] introduced the ship Energy Efficiency Design Index (EEDI) as a measure of ships CO_2 emissions, which, in the case of new built cargo ships (no ice-class), is calculated by the following formula:

$$EEDI = \frac{P_{ME} \cdot C_{FME} \cdot SFOC_{ME} + P_{AE} \cdot C_{FAE} \cdot SFOC_{AE} - f_{eff} \cdot P_{AEeff} \cdot C_{FAE} \cdot SFOC_{AE}}{Capacity \cdot V_{ref}} \qquad (18)$$

where EEDI is in g CO_2/t/NM, C_F is a conversion factor between fuel consumption (in g) and CO_2 emissions (also in g) and is based on fuel carbon content; C_F = 3.206 g CO_2/g fuel for the case of Diesel Gas/Oil and C_F= 2.750 g CO_2/g fuel for the case of LNG, ME and AE refer to the main and auxiliary engine(s), respectively; Capacity is taken the ship deadweight (DWT) for the cargo ships and the ship gross tonnage (GT) for the Ro-Pax ferries; PM_E is defined as the 75% of the rated installed power of the main engine after having deducted any installed shaft generator power; P_{AE} is the required auxiliary engine power to supply normal maximum sea load including necessary power for propulsion/machinery systems but excluding any other power e.g. ballast pumps, thrusters, cargo gear etc, in the condition where the ship engaged in voyage at the speed V_{ref} under the design loading condition; P_{AEeff} is the auxiliary power reduction due to innovative electrical energy efficient technology (e.g. WHR) measured at P_{ME}; f_{eff} is the availability factor of each innovative energy efficiency technology; $SFOC_{ME}$ and $SFOC_{AE}$ are the brake specific fuel oil consumptions (in g/kWh) of the main and auxiliaries engines at the 75% and 50% of their MCR points, respectively.

The baseline value of EEDI can be defined, based on regression analysis of data of several ships. For the case of RoRo cargo ships, the following expression was proposed [35]:

$$EEDI = 19788 \cdot DWT^{-0.714}$$ (19)

5. Financial evaluation of investments in maritime sector

The economic analyses of the alternative configurations for the ship propulsion plant are based on the calculation of the respective annual machinery cost, which consists of the Capital and the Operational expenditures. The Capital Expenditure (CAPEX) is the constant annual instalment to which the initial investment cost (IC) is equally distributed throughout the investment lifetime (n) under a determined discount rate (R) and can be calculated by the following equation given by VDI 2067 [36]:

$$CAPEX = IC \cdot R \cdot \frac{(1+R)^n}{(1+R)^n - 1}$$ (20)

The discount rate, which alternatively referred as the cost of capital, opportunity cost, or weighted average cost of capital, is used for spreading the investment cost over the expected investment life or it can be used for determining the present value of future benefits or costs. It can have a large impact on the results, and therefore, the selection of the proper value for the discount rate is important for accurately determining the capital expenditure. A minimum "risk free" discount rate values in the order of 4.0 to 4.5% for using in marginal abatement cost analysis of energy efficiency measures (including WHR) has been proposed in [37]. A discount rate value around 10% appears to be adequate for the cost analysis studies of marine industry.

The Operation Expenditure (OPEX) is the sum of the Annual Fuel consumption Cost (AFC) (including HFO, MDO and LNG), the Annual Lubricating Oil consumption Cost (ALOC), the Annual Maintenance Cost (AMC) and the Annual Urea solution consumption Cost (AUC) for the case where a SCR system is used. All those costs are calculated using main engine (subscript MEi) and auxiliary engines (subscript AEi) a) specific fuel oil consumptions for pilot - ($SFOC_{MEi}^{pilot}$, $SFOC_{AEi}^{pilot}$) and main fuel ($SFOC_{MEi}^{main}$, $SFOC_{AEi}^{main}$), b) specific lubricating oil consumptions ($SLOC_{MEi}$, $SLOC_{AEi}$), c) annual operating profile of the plant expressed in running hours (RH_{MEi}, RH_{AEi}) at certain load levels (P_{MEi}, P_{AEi}), d) fuel prices (FP^{pilot}, FP^{main}) , e) lube oil price (LOP), f) labour and parts prices expressed as specific maintenance cost (SMC_{MEi}, SMC_{AEi}), g) urea price (UP) and SCR system urea specific consumption (SUC_{MEi}, SUC_{AEi}). The OPEX is expressed by the following equation:

$$OPEX = AFC + ALOC + AMC + AUC$$ (21),

where:

$$AFC = FP_{pilot} \cdot \sum_{i=1}^{N} \left(SFOC_{MEi}^{Pilot} \cdot P_{MEi} \cdot RH_{MEi} + SFOC_{AEi}^{Pilot} \cdot P_{AEi} \cdot RH_{AEi} \right) +$$

$$FP_{main} \cdot \sum_{I=1}^{N} \left(SFOC_{MEi}^{main} \cdot P_{MEi} \cdot RH_{MEi} + SFOC_{AEi}^{main} \cdot P_{AEi} \cdot RH_{AEi} \right) \tag{22}$$

$$ALOC = \left(\sum_{i=1}^{N} \left(SLOC_{MEi} \cdot P_{MEi} \cdot RH_{MEi} + SLOC_{AEi} \cdot P_{AEi} \cdot RH_{MEi} \right) \right) \cdot LOP \tag{23}$$

$$AMC = \sum_{i=1}^{N} \left(SMC_{MEi} \cdot P_{MEi} \cdot RH_{MEi} + SMC_{AEi} \cdot P_{AEi} \cdot RH_{MEi} \right) \tag{24}$$

$$AUC = \left(\sum_{i=1}^{N} \left(SUC_{MEi} \cdot P_{MEi} \cdot RH_{MEi} + SUC_{AEi} \cdot P_{AEi} \cdot RH_{MEi} \right) \right) \cdot UP \tag{25}$$

where N is the number of operating conditions (i.e. sailing, manoeuvring, waiting in port).

6. Case Study

The ship investigated in this paper is a ferry or Ro-Ro cargo ship, whose general characteristics are presented in Table 1. The required ship propulsion power of 17 MW should be delivered by two four-stroke reciprocating engine units of 8.5 MW (or more), whereas three generating sets of 1 MW power are required for covering the ship electric energy demand. The ship is considered to sail in a route of 1160 NM, which includes a part of 340 NM inside ECA. An example of this route is the itinerary between the ports of Trieste (Italy) and Istanbul (Turkey). Each leg of ship voyage lasts approximately 58 h considering a sailing speed of 20 knots; 57 h sailing and 0.5 h manoeuvring time at each port. It is also assumed that the ship stays 7 h on each port of her voyage and operates 80% of the calendar year. In specific, the ship spends her annual operating hours, as follows: 5.4% in ECA Ports, 5.4% in Non-ECA Ports, 0.39% manoeuvring in ECA waters, 0.39% manoeuvring in Non-ECA waters, 25.9% sailing in ECA open sea and 62.5% sailing in Non-ECA open sea.

The following alternative propulsion plants are investigated in the present study: a) The vessel is equipped with two medium speed diesel engines for propulsion and three diesel generating sets (for example the W9L46 marine Diesel engine [38] and the W6L20 generating set [39] respectively, both from Wärtsilä), running on Marine Gas Oil (MGO) within ECA zones and on Low Sulphur Heavy Fuel Oil, outside ECA zones. A selective catalytic reduction system (SCR) is considered to be installed for reducing NOx emissions when the ship operates within ECA zones (fulfillment of IMO Tier III emission level). The SCR system is consuming urea solution and is switched off when the Ferry is sailing in Non-ECA zones, where the less strict NOx emission levels (IMO Tier II) can be met by the engines, without any exhaust gas after-treatment system. b) The vessel is equipped with two medium speed dual fuel engines for propulsion and three dual fuel generating sets (for example the W9L50DF [40] dual fuel marine engine and the W9L20DF dual fuel generating set [39] respectively, both from Wärtsilä), continuously running on LNG. A small amount (around 1% on energy basis) of MGO is also

injected in engines cylinders for combustion commencement. The combustion of LNG enables the engines to meet the emission limits inside and outside ECA zones. c) This configuration is as the case (a) with the addition of a waste heat recovery system (WHR), recovering energy from the main engines exhaust gases for producing superheated steam, to be expanded in a steam turbine coupled to an electric alternator. d) This configuration is as the case (b) with the addition of the waste heat recovery system described above. The advantage of the configurations with WHR systems is that electricity can be generated onboard by the turbo-generators, enabling the ship operator to unload or even switch off one of the ship generating sets. The main engine parameters of the selected Diesel and DF engines are given in Table 2.

Table 1. Ferry Main Particulars

Characteristic	Value
Size	35000 GT
Length	220 m
Beam	28.2 m
Draft	7.0 m
Speed (service)	21.0 knots
Deadweight	12500 mt
Propulsion Power (installed)	17.0 MW
Aux. Power (installed)	3.0 MW
Propulsion	2 CP propellers

Table 2. Main Engine Parameters

Characteristic	Diesel Engine	Dual Fuel Engine
Cylinders	9L	9L
Bore	460 mm	500 mm
Stroke	580 mm	580 mm
Brake Power at MCR	8775 kW	8775 kW
Brake Power at MCR	500 rpm	514 rpm

The required engine data for modelling the WHR system include the mass flow rate, temperature and equivalence ratio of the exhaust gas exiting engine turbocharger turbine. The latter was used for estimating the exhaust gas composition considering perfect combustion, which, in turn, was used for calculating the exhaust gas specific heat at constant pressure. For the case of the heating the feed water using the engine air cooler, the temperature of the air exiting the turbocharger compressor is also required as input. All the required parameters are taken for engine loads in the range from 50% to 100% of MCR, considering that the engines operate according to propeller law and ISO ambient conditions, using the data given in the engine project guides [38-40]. An increase by 3% for the reported values brake specific fuel consumption was taken into account since the manufactures give the engine BSFC values with a tolerance of ±5%. The shafting system efficiency for all the examined cases is considered to be 97% at MCR, whereas the correction that is given in [34] is taken in to account at lower engine loads.

For the case of 9L46 engine operating at MCR, an exhaust gas amount of 30% was considered to bypass the boiler, so that the boiler geometric characteristics are kept balanced. This value derived

considering that the available engine exhaust energy at 100% load is approximately 30% greater than the one for the case of 85% load. Thus, the oversizing of the exhaust gas boiler is avoided, since the engine rarely operates at 100% load. For the case of the diesel engines, the urea flow rate was calculated using the equation reported in [9] considering a 40 wt % urea-water solution and exhaust gas NOx emission level of 2.5 g/kWh to comply with Tier III limits. The LNG fuel composition was taken as follows: 95% methane, 2% ethane and 3% butane; the lower heating value of that LNG was calculated to be 49467 kJ/kg.

The values of the temperature and mass flow rate of the exhaust gas exiting the engine for both the examined engines (9L46 running on MDO and 9L50DF running on LNG and using MDO pilot injection for the start of combustion) as well as the exhaust gas thermal power, which are used in the WHR installation simulation cases presented below, are shown in Figure 3. The brake efficiency for both engines as well as the product of engine brake efficiency and the shafting system efficiency are also given in Figure 3. The DF engine operates with increased efficiency 2-3% for the load region from 85% and above compared to the diesel engine. Although, the exhaust gas mass flow rates of both engines are comparable, the exhaust gas waste thermal power are greater for the case of the dual fuel engine due to the exhaust gas higher temperature values in the region from 55% to 95% of engine load.

A set of results including the net produced electric power, the power plant efficiency increase due to the production of the electric power from the WHR system, the total power plant efficiency and the minimum temperature difference at exhaust gas boiler pinch point for the cases of the 9L46 and 9L50DF engines are presented in Figure 4. The following cases for the WHR system parameters were simulated: no heating of the feed water tank and heating the feed water using the engine air cooler. In all the simulated cases, no production of saturated steam for the ship heating services was assumed. The boiler drum absolute pressure was considered to be 8.5 bar, whereas the pressure of the condenser was taken as 0.065 bar. The temperature-heat transfer rate diagrams of the exhaust gas boiler for the 9L46 engine operating at 85% load for the case of no heating the feed water tank and heating the feed water tank using the engine air cooler are shown in Figure 5.

As it can be deduced from Figure 4, a considerable amount of electric power is produced, namely from 350 kW to 490 kW for the case of 9L46 engine and from 350 kW to 640 kW for the case of 9L50DF engine. In the case of the dual fuel engine, the produced electric power is greater by 100 to 120 kW when the engine operates at load region from 70% to 100% of MCR. This means that in the case of simultaneous operation of both ship main engines at 75% load, the respective exhaust gas WHR systems can generate 800 kWe for the case of Diesel engines and 1040 kWe for the case of DF engines. Therefore, in the latter case, one of the ship generating sets can be switched off. The efficiency increase owing to the net electric power generation (the power required by the WHR system pumps are excluded) is above 2.5% for the case of 9L46 engine and above 3.2% for the case of the 9L50DF engine, which indicates that the power plant efficiency is substantially improved when a WHR system is used. The power plant total efficiency (the product of engine brake efficiency and the shafting

system efficiency plus the efficiency increase) is in the range of 48 to 49% for the case of the 9L46 engine, whereas it can reach values as high as almost 52% in the case of the 9L50DF engine. Therefore, it is estimated that even in the case of using dual fuel-electric propulsion, the overall propulsion system efficiency can be maintained in comparable levels to a conventional Diesel engine propulsion system, taking into account the respective propulsion systems losses (3% for the case of a conventional four-stroke Diesel engine propulsion system vs. 10% for the case of the dual fuel engine-electric propulsion system, both at MCR).

The minimum exhaust gas boiler temperature difference (pinch point) is maintained above 10°C for the case of the 9L46 engine and above 15°C for the case of 9L50DF engine, which means that the exhaust gas boiler for the case of DF engine will be less bulky, since smaller heat transfer area is required. This is explained by considering the temperature profiles of both engines shown in Figure 3. For the DF engine, the exhaust gas temperature lays in the region from 370°C to 390°C with the lower temperature obtained at 100% engine load. At that load, the minimum temperature difference is slightly above 15°C. On the other hand, for the Diesel enginethe minimum temperature of the exhaust gas is obtained for the operating point of 85% load. At that point, the minimum temperature difference if slightly above 10°C.. In the case of heating the feed water using the engine air cooler, the heat transfer rate of the economiser section of the exhaust gas boiler is lower, having, as a result, the reduction of the minimum temperature difference. Thus, higher temperature of the exhaust gas exiting the boiler is required in order to maintain the minimum temperature difference at acceptable level. This is clearly seen in Figure 5 comparing the left and right diagrams. The exhaust gas temperature at boiler exit is increased by 10°C in the case of heating the feed water using the engine air cooler (Figure 5b), so that the temperature difference at pinch point is kept above 10°C. For that reason, the electric power production for the WHR system with the feed water heating using the engine air cooler is only marginally improved in comparison to the feed water no heating case. In that respect, the heating of feed water using the engine air cooler seems not to be a viable option for case of a single pressure WHR system.
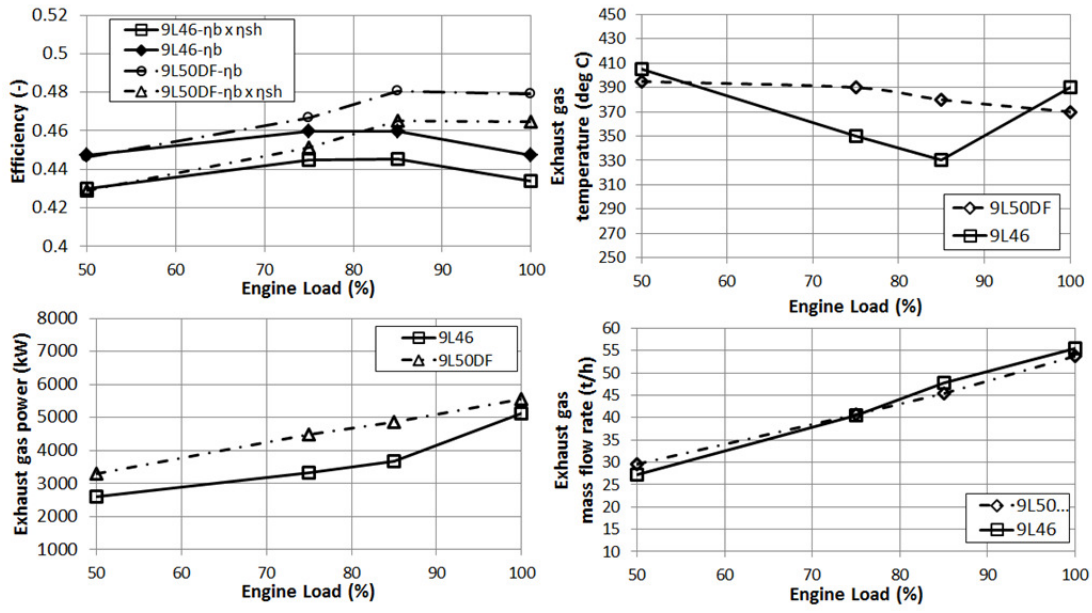
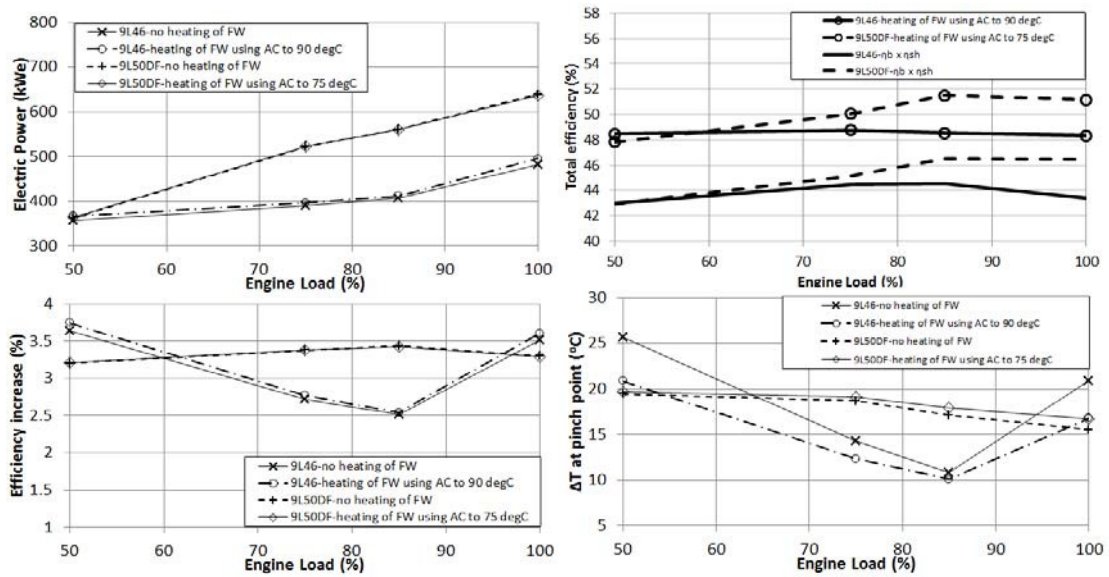Figure 3. Engine exhaust gas parameters as functions of engine load

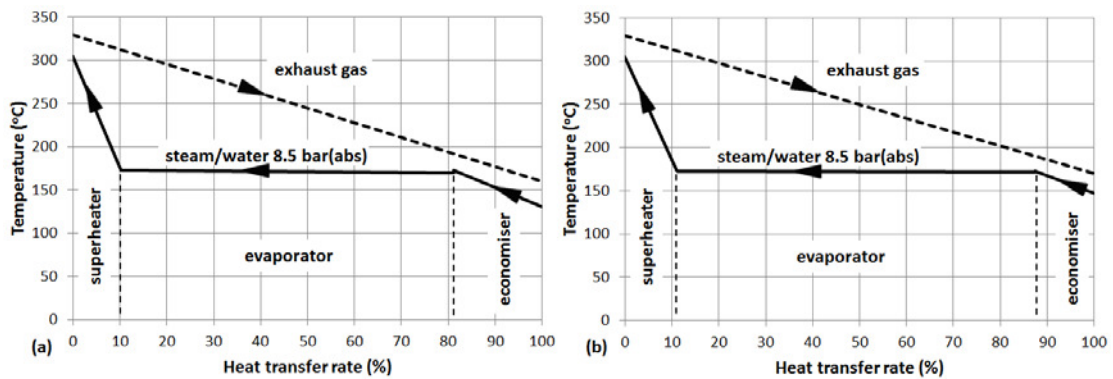Figure 4. WHR system parameters for the examined engines

Figure 5. Temperature-Heat transfer rate diagrams for the exhaust gas boiler of the 9L46 engine operating at 85% load for the cases of (a) no heating the feed water and (b) heating the feed water using the engine air cooler to 90°C

The attained Energy Efficiency Design Index (EEDI) was calculated using equation (5) considering the Ro-Ro cargo ship case for the various options of its propulsion plant installation (diesel engine with and without WHR, Dual Fuel engine with and without WHR). The derived results are presented in Figure 6. As it can be observed, the calculated EEDI value for the case of Diesel engines propulsion plant is 32.4, whereas the EEDI for the case of LNG (Dual Fuel) engines propulsion plant is 23.7. Both values are greater than the proposed baseline EEDI value, which was found 23.5 according to equation (6). Thus, it is inferred that even in the case of using a "clean fuel" such LNG, the attained EEDI marginally exceeds the EEDI baseline value. This means that only the change of fuel is not adequate for complying with the EEDI regulations, and therefore, additional measures should be taken for increasing the ship propulsion plant efficiency in the design phase. The installation of a WHR system belongs to the possible solutions. In such a case, significant reductions of the attained EEDI can be obtained; from 32.4 to 30.9 for the case of Diesel engines; from 23.7 to 21.2 for the case of DF engines. However, as it is also observed from Figure 6, only the combination of LNG and WHR can obtain EEDI value below the baseline limit and in that respect it can be regarded as completely green alternative propulsion plant according to the imposed IMO EEDI regulations.

The economic viability of this option will be investigated below based on figures presented in recent publications of [18], [19] and [21]. The machinery costs estimations for each one of the ship propulsion plant alternatives are given in Table 3. The annual machinery costs were calculated for each propulsion plant alterative, considering 55 roundtrips per year, HFO price 483 €/t, MDO price 676 €/t, LNG price 477€/t, Urea Price 350€/t, a discount rate of 10% and duration of investment 20 years. The results are presented in Figure 7. As can be observed from Figure 7, there are significant savings when a WHR system is added. In detail, the savings found to be 391.1 k€/year for the case of the Diesel engines and 801,8 k€/year for the case of the LNG engines. It must be noticed that the optimum solution remains the "LNG-WHR" propulsion plant with around 2,4 M€ annual savings compared with the "Diesel–WHR" propulsion plant. This means that the LNG engines combined with a WHR system, despite of the increased cost of initial investment, remain the most cost effective solution and in the same time environmentally sound.
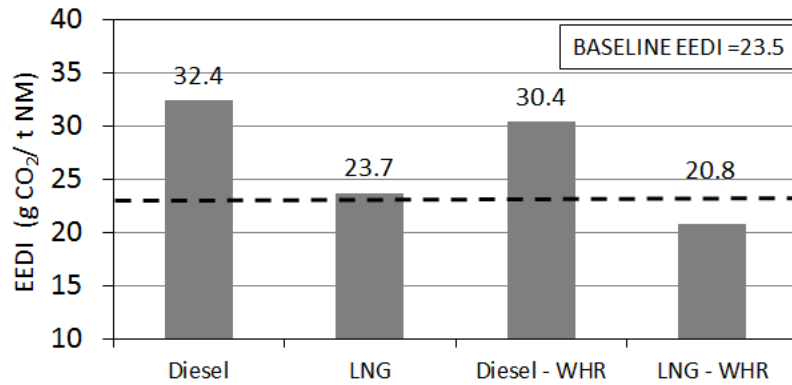
Figure 6. Calculated Energy Efficiency Design Index (EEDI) for the investigated alternative propulsion plants
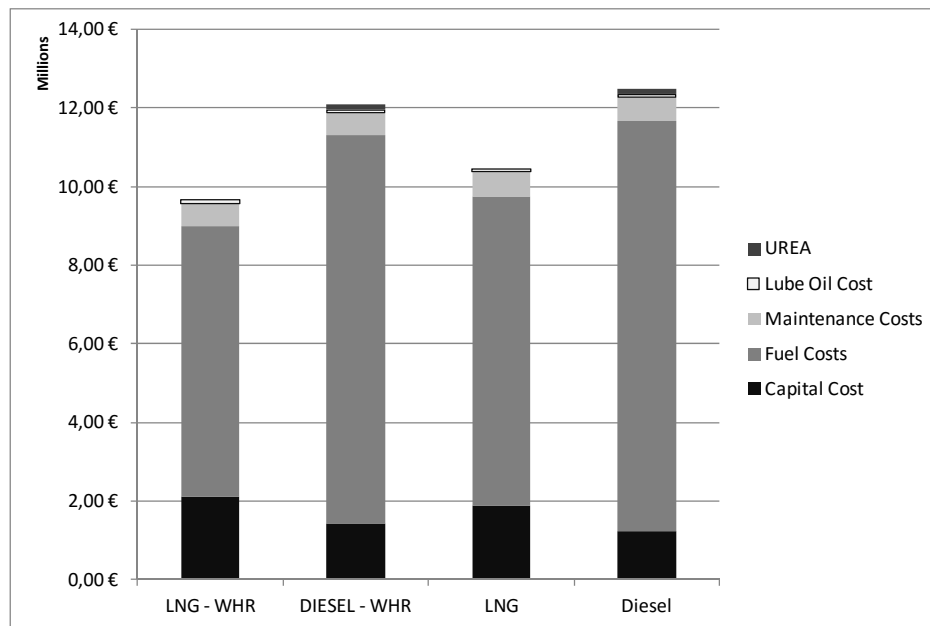
Figure 7. Annual Machinery Costs

Table 3. Specific Machinery Costs

Machinery Item	Cost (EUR/kW)
Main Engine (Diesel)	235.00
Propulsion Line	220.00
Generating Sets	505.00
SCR system	40.00
LNG Tanks and Equipment	365.00
Waste Heat Recovery System	103.00

7. Conclusions

The techno-economic sustainability of four alternative propulsion plants, based on reciprocating internal combustion engines running either on Diesel or LNG fuels, equipped or not with Waste Heat Recovery systems was investigated for the of a typical ferry or Ro-Ro ship operating in a route passing through ECA. The main findings derived from this work are summarised as follows.

The ship propulsion plant comprising by DF engines and running on LNG can operate with up to 2% higher efficiency compared to the diesel engines propulsion plant. When a WHR system is used for generating electric power, a substantial part of the ship electric energy demand can be covered. In the case of LNG propulsion, a 3.2 to 3.5% increase in the plant efficiency was calculated, whereas the predicted efficiency increase was from 2.5 to 3.5% in the case of diesel propulsion. More electric power can be produced for the case of LNG propulsion. When both DF engines operate at 85% load, the switching off of one of the generating sets is possible. For the examined single steam pressure WHR system, the option of heating the feed water by using the engine air cooler stages does not significantly improve the overall system efficiency, and hence, it is not considered as a viable solution, as it can be for the WHR systems of double steam pressures.

For the Ro-Ro ship case, the diesel engines propulsion plant, even in the case where the WHR system is installed, presented EEDI values above the proposed baseline. The DF engines propulsion plant EEDI is in the region of the proposed baseline value (although slightly above). Only the combination of DF engines and WHR demonted an EEDI value lower than the proposed baseline, indicating that additional measures should be taken, so that a new built ship comply the EEDI legislation.

The economic analysis of the examined options demonstrated that although the DF engines propulsion plant has greater initial cost, it gave lower annual cost, which is attributed to the higher overall efficiency and the lower price of LNG compared with the MDO/MGO price. The inclusion of WHR system further lowers the propulsion installation annual machinery cost. However, it must be noted that the possible reduction of the transport ship capacity due to the increase volume of the LNG fuel storage system was not taken into account in the present analysis.

In conclusion, the solution of the DF main engines running on LNG combined with a WHR system for electricity generation was found to be technically, environmentally and economiclly sound, by reaching the higher total energy efficiency up to 52%, the lower EEDI value (20.8) (below the limit of 23.5 for the Ro-Ro ship case), 80% less NOx emissions, practically no sulphur emissions and a superior cost effectiveness proved by annual saving in operating costs exceeding 2 M€ compared with the Diesel engines alternative for the examined ship operational profile.

However, several challenges related with the use of LNG onboard, should be seriously taken into consideration, before the final selection is made. The lack of LNG infrastructure in the majority of the commercial ports, the limited experience from running marine engines with gas fuels, the required safety measures, the future gas price variation are among the critical factors that should be further investigated in the future works.

References

[1] IMO. 2011, Resolution MEPC.203(62), Amendments to the annex of the protocol of 1997 to amend the international convention for the prevention of pollution from ships, 1973, as modified by the protocol of 1978 relating thereto (Inclusion of regulations on energy efficiency for ships in MARPOL Annex VI), MEPC 62/24/Add.1, London: International Maritime Organization.

[2] IMO. 2012, a) Resolution MEPC.212(63) Guidelines on the method of calculation of the attained energy efficiency design index (EEDI) for new ships. MEPC 63/23, London: International Maritime Organization.

[3] IMO. 2012, b) Resolution MEPC.213(63), Guidelines for the development of a ship energy efficiency management plan (SEEMP), MEPC 63/23, London: International Maritime Organization.

[4] IMO, Sulphur oxides (SOx) – Regulation 14, London: International Maritime Organization.

[5] IMO, Nitrogen Oxides (NOx) – Regulation 13, London: International Maritime Organization.

[6] Levander, O. (2009) New Concepts in Ferries propulsion, Wärtsilä Publication, 01/2009, pp. 1-11.

[7] Wik, Ch. (2013) Tier III technology development and its influence on ship installation and operation, In Proceedings of the 27th CIMAC World Congress. Shanghai. China. 13–16 May 2013. Paper No: 159.

[8] MAN Diesel and Turbo. (2008) Exhaust Gas Emission Control Today and Tomorrow-Application on MAN B&W Two-stroke Marine Diesel Engines, Publ. No. 5510-0060-00, Copenhagen, Denmark.

[9] Wärtsilä. (2013) Wärtsilä environmental product guide, Issue 2/2013, June 2013, Wärtsilä Finland Oy.

[10] Wood, DA. (2012) A review and outlook for the global LNG trade, Journal of Natural Gas Science and Engineering, 9. 16-27.

[11] Bengtsson, S. Andersson, K & Fridell, E. (2011) A comparative life cycle assessment of marine fuels: liquefied natural gas and three other fossil fuels, Proc IMechE, Part M: J of Engineering for the Maritime Environment, 225, 97-110.

[12] Hoenders, R., EU Initiatives regarding the use of LNG as bunker fuel and EMSA's involvement in promoting the use of LNG as alternative fuel, European Maritime Safety Agency (EMSA), July 2013,

[13] DMA. (2012) North European LNG Infrastructure Project A feasibility study for an LNG filling station infrastructure and test of recommendations, March 2012, Copenhagen: The Danish Maritime Authority.

[14] Adreola, M. & Tirelli, G. (2007) Dual-fuel-electric LNG carrier machinery: when a concept becomes reality, Wärtsilä Technical Journal: Marine/InDetail, 02/2007, 33-36.

[15] Woodyard, D. (2009) Pounders Marine Diesel Engine and Gas Turbines, 9th ed. Elsevier Ltd, Oxford, UK.

[16] Murukami, S. & Baufeld, T. (2013) Current status and future strategies of Gas Engine Development, In Proceedings of the 27th CIMAC World Congress. Shanghai. China. 13–16 May 2013. Paper No: 413

[17] Dirix, T. (2013) Operational experiences of DNV classed Gas Fuelled vessels, In Proceedings of the 27th CIMAC World Congress. Shanghai. China. 13–16 May 2013. Paper No: 158.

[18] Bui, Y. (2011) Machinery Concepts and LNG for meeting IMO Tier III rules, Wärtsilä Technical Journal: Marine/InDetail, 01/2011, pp. 31-38.

[19] Levander, O. (2011) Handy Size LNG Cruise Ship Concept, Wärtsilä Technical Journal: Marine/InDetail, 01/2011, pp. 44-51.

[20] MAN Diesel and Turbo. (2005) Thermo Efficiency System (TES) for Reduction of Fuel Consumption and CO_2 Emission, Publ. No.: P3339161, Copenhagen, Denmark.

[21] MAN Diesel and Turbo. (2011) MAN Diesel and Turbo Technology Boosts Efficiency-WHR and TCS-PTG improve efficiency on large engines, Publ. No.: 6510-0238, 6/2011, Copenhagen, Denmark.

[22] Schmid, H. (2004) Less emissions through waste heat recovery, Green Ship Technology Conference, London, 28-29 April 2004, London, UK. SNAME. (1990) Marine Diesel Power Plant Practices, T&R Bulletin 3-49.

[23] Shu, G. Liang, Y., Wei, L. Tian, H. Zhao, J. & Liu, L. (2013) A review of waste heat recovery on two-stroke IC engines aboard ships, Renewable and Sustainable Energy Reviews, 19, 385-401.

[24] Dimopoulos, G.G. Georgopoulou, Ch.A. & Kakalis, N.M.P. (2011) Modelling and optimisation of an integrated marine combined cycle system. In Proceedings of ECOS 2011 Conference, Novi Sad, Serbia, July 4–7 2011, 1283-1298.

[25] Hountalas, DT. Katsanos, C & Mavropoulos G C. (2012) Efficiency improvement of large scale 2-stroke Diesel engines through recovery of exhaust gas using Rankine cycle, Procedia-Social and Behavioral Sciences, 48, 1444-1453.

[26] Choi, BC. & Kim, YM. (2013) Thermodynamic analysis of a dual loop heat recovery system with trilateral cycle applied to exhaust gases of internal combustion engine for propulsion of the 6800 TEU container ship, Energy, 58, 404-416.

[27] Gewald, D. Karellas, S. Schuster, A. & Spliethoff, H. (2012) Integrated system approach for increase of engine combined cycle efficiency, Energy Conversion and Management, 60, 36-44.

[28] Burel, F. Taccani, R. Zuliani, N. (2013) Improving Sustainability of Maritime Transport through utilization of Liquefied Natural Gas (LNG) for Propulsion, Energy, 57, 1, pp. 412–420.

[29] Theotokatos, G. & Livanos, G. (2013) Techno-economical analysis of single pressure exhaust gas waste heat recovery systems in marine propulsion plants, Proc IMechE Part M: J Engineering for the Maritime Environment, 227(2), pp. 83–97.

[30] Theotokatos, G. (2010) On the cycle mean value modelling of a large two-stroke marine diesel engine, Proc. IMechE Part M: J. Engineering for the Maritime Environment, 224, pp. 193-205.

[31] Kyrtatos, N.P. Theodossopoulos, P. Theotokatos, G. & Xiros, N. (1999) Simulation of the overall ship propulsion plant for performance prediction and control, In Proceedings of the Conference on Advanced marine machinery systems with low pollution and high efficiency (MarPower '99), 25–26 March 1999, Newcastle upon Tyne, UK.

[32] Rakopoulos, CD. & Giakoumis EG. (2006) Review of thermodynamic diesel engine simulations under transient operating conditions. Trans SAE, J Engines, 2006; 115: 467–504 [SAE paper no. 2006-01-0884].

[33] Livanos, G.A. Simotas, G.N. & Kyrtatos, N.P. (2006) Tanker Propulsion Plant Transient Behavior during Ice Braking Conditions, 16th International Offshore and Polar Engineering Conference (ISOPE 2006), San Francisco, USA.

[34] SNAME. (1990) Marine Diesel Power Plant Practices, T&R Bulletin 3-49.

[35] IMO. (2009) Recalculation of energy efficiency design index baselines for cargo ships, GHG-WG 2/2/7.

[36] VDI 2067, (2000), Wirtschaftlichkeit gebaudetechnischer Anlagen: Grundlagen der Kostenberechnung.

[37] Russel, B. & Amand, D. (2011) Marginal Abatement Costs and Cost Effectiveness of Energy Efficiency Measures, SNAME T&R Program, Panel AHP 20: Greenhouse Gases & Economics, March 2011.

[38] Wärtsilä. (2007) Wärtsila 46 product guide, 3/2007, Finland.

[39] Wärtsilä. (2012) Wärtsila 20DF product guide, 7/2012, Finland.

[40] Wärtsilä. (2011) Wärtsila 50DF product guide, 2/2011, Finland.

.

Nomenclature

AE	specific available energy (J/kg)
AFC	annual costs for fuel consumption (€)
AK	annual machinery cost (€)
ALOC	annual lubricating oil consumption costs (€)
AMC	annual maintenance cost (€)
AUC	annual urea consumption cost (€)
c_p	specific heat at constant pressure (J/kg/K)
c_u	urea concentration (%)
C_F	conversion factor (g CO_2/g fuel)
CAPEX	capital expenditure (€)
DWT	deadweight (t)
EEDI	Energy Efficiency Design Index (g CO_2/t/NM)
FP	Fuel Price (€/g)
f	correction factors (-)
h	specific enthalpy (J/kg)
H_L	lower heating value (J/kg)
IC	investment cost (€)
IRR	internal rate of return (%)
LOP	lube oil price (€/g)
$\dot{m}$	mass flow rate (kg/s)
n	lifetime of investment (years)
OPEX	operation expenditure (€)
P	power (W)
$\dot{Q}$	heat transfer rate (W)
R	discount rate (-, %)
RH	Running Hours
SFOC	brake specific fuel consumption (g/kWh)
SLOC	brake specific lubricating oil consumption (g/kWh)

SMC	specific maintenance cost (€/kWh)
SUC	specific urea consumption (g/kWh)
T	temperature (K)
UP	urea price (€/g)
V_{ref}	reference ship speed (kn)
$\overset{.}{V}$	volumetric flow rate (W)
ε	heat exchanger effectiveness (-)
η	efficiency (-)
ΔNOx	specific NOx emissions reduction (g/kWh)
Δp	pressure drop, pressure increase (Pa)
ΔT	temperature difference (K)
Δη	efficiency increase (-)
ρ	density (kg/m^3)

Subscripts

a	air
ac	air cooler
AE	auxiliary engine
b	boiler
bv	baseline value
c	condensate water
cw	circulating water
d	drum
ec	economizer
el	electric
ev	evaporator
f	fuel
fw	feed water
g	exhaust gas
G	generator

hfw	heating of feed water
HT	high temperature
i	inlet
is	isentropic
m	mechanical
ME	main engine
o	outlet
pd	pump downstream
pp	pinch point
pu	pump upstream
s	saturated steam
sh	superheater, superheated steam
ST	steam turbine
sw	sea water
TG	turbogenerator
u	urea
w	saturated water

Abbreviations

AE	auxiliary engine(s)
CO_2	carbon dioxide
EIAPP	Engine International Air Pollution Prevention
HFO	heavy fuel oil
IMO	International Maritime Organization
LNG	liquefied natural gas
LPG	liquefied petroleum gas
MCR	maximum continuous rating
MDO	marine diesel oil
ME	main engine(s)
MGO	marine gas oil

NOx   nitrogen oxides

SCR   selective catalytic reactor

SOx   sulphur oxides

WACC   weighted average cost of capital

WHR   waste heat recovery